BARTOSZ PRZYSUCHA

Lublin University of Technology, Poland

ORCID iD: orcid.org/0000-0002-1117-8088

MARCIN KOWALSKI

WSEI University in Lublin, Poland

ORCID iD: orcid.org/0000-0002-1644-0612

MICHAŁ OLESZEK

Netrix S.A., Poland

ORCID iD: orcid.org/0000-0002-8979-9650

MARIUSZ SUTRYK

WSEI University in Lublin, Poland

ORCID iD: orcid.org/0000-0002-8998-125X

MEASUREMENT CHANNELS' INFORMATION RELATIONSHIPS IN BODY SURFACE POTENTIAL MAPPING

RELACJE INFORMACYJNE KANAŁÓW POMIAROWYCH W MAPOWANIU POTENCJAŁU POWIERZCHNI CIAŁA

ABSTRACT

Body Surface Potential Mappings (BSPM) measurements allow heart rate monitoring. Based on measurements obtained from BSPM, defects and heart rhythm disorders can be detected. Due to the multitude of data obtained from BSPM measurements, the crucial aspect in the potential test signals analysis on the human body is the automation of the disturbance detection process. This automation process involves the use of advanced algorithms and machine learning techniques to analyze the recorded data and identify patterns indicative of heart rhythm disorders. In the article, the information dependencies in the measurement channels were analyzed and presented. PCA analysis was used to determine informational relationships between the channels. The study was carried out on the data from simulations made for the BSPM measuring vest on a simulation system created for this purpose and based on the ECG signal generator. As a result of the conducted research indicated informational relationships between the channels for signals with disturbances: Atrial fibrillation, Brachycardia, Normal signal, PVC, Tachycardia, Ventricular Fibrillation, and Ventricular Tachycardia.

STRESZCZENIE

Pomiary BSPM (Body Surface Potential Mappings) umożliwiają monitorowanie rytmu serca. Na podstawie pomiarów uzyskanych z BSPM można wykryć wady i zaburzenia rytmu serca. Ze względu na mnogość danych uzyskiwanych z pomiarów BSPM, kluczowym aspektem analizy potencjalnych sygnałów testowych na ludzkim ciele jest automatyzacja procesu wykrywania zakłóceń. Automatyzacja ta polega na wykorzystaniu zaawansowanych algorytmów i technik uczenia maszynowego do analizy zarejestrowanych danych i identyfikacji wzorców wskazujących na zaburzenia rytmu serca. W artykule przeanalizowano i przedstawiono zależności informacyjne w kanałach pomiarowych. Do określenia zależności informacyjnych pomiędzy kanałami wykorzystano analizę PCA. Badania przeprowadzono na danych pochodzących z symulacji wykonanych dla kamizelki pomiarowej BSPM na stworzonym w tym celu systemie symulacyjnym opartym na generatorze sygnału EKG. W wyniku przeprowadzonych badań wskazano zależności informacyjne pomiędzy kanałami dla sygnałów z zaburzeniami: Migotanie przedsionków, Brachykardia, Sygnał prawidłowy, PVC, Tachykardia, Migotanie komór i Częstoskurcz komorowy.

KEYWORDS: *BSPM measurements, Principal component analysis, heart disease classification, vest for BSPM measurement, areas of BSPM heart activity*

SŁOWA KLUCZOWE: *Pomiary BSPM, analiza składowych głównych, klasyfikacja chorób serca, kamizelka do pomiaru BSPM, obszary aktywności serca BSPM*

Introduction

ECG examination is a primary diagnostic procedure for detecting heart rhythm disorders. It is based on the electrical potential analysis at ten measurement points (leads/electrode). It is possible to identify distortions in the ECG signal characteristic of different abnormalities using diagnostic charts obtained from measurements. Some defects require the connection of a heart rate monitor for a more extended period. Automation of the analysis process and automatic detection allow for efficient analysis of large amounts of recorded data during extended measurements (Przysucha, 2020; Kłosowski, 2020).

It is difficult to continuously detect abnormal heart rhythms automatically. Measurement must be performed to minimise uncertainty related to the poor contact between the electrode and the body. We also need to be able to correct signals affected by static electricity generated by the patients' clothes.

To improve the measurements, an electrical potential is measured on the entire chest (Robinson and Curzen, 2009). Such a method is called Body Surface Potential Mapping (BSPM) and has been done with 62 or 102 electrodes in the past (Rodrigo, 2017). This research has been carried out since the 1960s (Lux, 2010, Polak-Jonkisz, 2009). However, only in connection with machine learning and the rising computing power of machines can research on the automatic classification of disturbances be conducted (Polak-Jonkisz, 2009; Hoekema, 2004; Hänninen, 2003; SippensGroenewegen, 2000; Rymarczyk, 2020).

The possibilities of BSPM are much more extensive compared to classical ECG tests (Korhonen, 2009; Simelius, 2003). In BSPM, obtaining the potential from electrodes placed on the entire chest is possible. The most critical are the channels placed at the heart level in front and the back of the chest. They allow for the data acquisition of heart activity from the back walls of the ventricles. Data from these regions is valuable for detecting abnormalities such as coronary artery seaside or past myocardial infarctions (Zarychta, 2007). The BSPM was also helpful in diagnosing acute coronary artery occlusion (Daly, 2013).

The problem of investigating the information dependence of BSPM measurement signals has been raised in many papers. However, the studies were usually limited to a particular disease entity. For instance, in (Weber, 2011), the authors focused on determining a representative set of latent variables

(Principal Components) for modifications caused by changes in tissue conductivity. Latent variables were defined for blood, skeletal muscle, lung and adipose tissue changes. In (Mark Potse, 2017), a study was carried out on the analysis of PCA for Ventricular Fibrillation disorder for measurements where sampling took place every half second. Three latent variables were selected to represent a set of measurement signals. The work (Bonizzi, 2009) focused on PCA analysis for Atrial Fibrillation disorder. The results of PCA analysis were used to classify cases with and without the disorder. In a paper (Donnelly, 2006), signal measurements from patients with old inferior myocardial infarction and healthy persons were examined. First, PCA was used to reduce the dimensions of the measurement space. Then, based on the obtained latent variables, case classification was performed. There are also many papers about PCA in ECG, for example (Castells, 2007).

The main aim of the research is to verify and indicate the advantages of PCA analysis in detecting heart diseases, especially in the context of the classification of ECG signals. The paper addresses the issue of determining and comparing latent variables for a large class of illnesses by identifying locations on the patient's body connected with latent variables obtained through PCA analysis. This information may be beneficial in the event of examinations utilizing, for example, 12-channel ECGs, in which the areas responsible for recognising the disease entity are positioned in a different location than the electrodes used in a conventional ECG. Moreover, this manuscript discusses the issue of information reliance between channels and identifies the importance of analysis of BSPM data during measurements to detect invalid measurements. Understanding the mechanics of electrical potential diffusion in the patient's body requires understanding information linkages.

This research provides a starting point for clinical studies related to the testing of the BSPM measurement vest. Knowing the information dependencies created as a result of performing the PCA analysis on simulation data, there is a possibility of verifying measurements from patients and detecting defects of the measurement system or noise possibly occurring in the measurement path. The information relations in PCA channels performed on simulation data and, thus, on model data will enable the validation of the operation of the measuring system. In case of faulty signal registration from a particular

electrode or signal disturbances, the information relations between the channels resulting from the conducted PCA analysis will be disturbed. The research was conducted using data simulated from the certificated ECG simulator. The simulation system was created as a part of the test mechanism for the designed BSPM vest with 102 electrodes. The conducted tests showed that the reduction of PCA dimensions increases classification efficiency through the increased ability of the model to reduce noise and increase classification speed. A not insignificant advantage of the complexity reduction achieved by using PCA is the simplification of the BSPM system design (both hardware and software), which, in the case of commercialisation of the tested solution, positively affects the price competitiveness of the device.

This manuscript is an expansion of the study (Wójcik, 2022). In particular, the described research was performed using an upgraded phantom. In the survey (Wójcik, 2022), the measuring hardware was directly connected to resistor mesh, while in the work presented in this paper, we use a much more sophisticated fandom where with a mannequin torso with a copper imitation of human skin and textile electrodes Improved hardware was also used. The differences include a new filtering system and communication protocols inside the measuring board.

The work presented in this paper is part of a project whose primary goal is to develop a mobile tomographic system for 3D imaging of the heart and lungs using BSPM and electrical impedance tomography (EIT).

Our system is divided into two significant parts: the mobile measuring device and the intelligent cloud framework (Rymarczyk, 2019). The main module is an integral section of the mobile measuring device. Its functionality includes acquiring and preliminary processing of measurement data, calibrating active electrodes, sending the data to the web-server system, and powering the entire system. The data acquisition device (DAD) consists of intelligent clothing monitoring vital signs. It performs ECG measurements through the body surface potential mapping (BSPM) and electrical impendence tomography (EIT) and thus monitors the lungs. This wearable system is designed in such a way that it does not constrain the movement of the patient while at the same time taking reliable data. At the moment, the garment is equipped with 102 electrodes. The 32 are arranged in two rows (16 electrodes in each row) and

distributed uniformly in a plane around the chest perimeter. These electrodes are used for the EIT measurements. The rest of the electrodes are being used for BSPM. The second part of the DAD is the electronics connected to the electrodes responsible for sensing, filtering, and amplifying biosignals. The sensing analogue front-end unit amplifies biosignals to the analogue-to-digital converters (ADCs) level, and preliminary filtering is required. The digital processing part is a chip (SoC) system consisting of a field-programmable gate array (FPGA), microcontroller, and wireless communication modules, such as BT/BLE and Wi-Fi.

The system also contains algorithms for image reconstruction for a human chest model with lungs and heart. Electrical impedance tomography was used for this purpose. It is a non-invasive imaging method involving examining an unknown object using electric currents and appropriate measurements of voltage drops at its edge. In medical clinical trials and practice, imaging has become an essential part of diagnosing and studying the anatomy and function of the human body. The fusion of complementary methods will significantly improve diagnostic capabilities. The measurement modules implemented in the portable device, namely electrical impedance tomography and body surface potential mapping, will track lung ventilation and cardiac activity in real-time.

The system will be a world novelty in terms of functionality and the development and application of technological solutions. The main novelty of this paper is the construction of the new hardware with a unique filtering and measuring setup capable of measuring not only the BSPM signal but also 3D electrical impedance tomography (EIT). The solution is based on a custom application of the FPGA.

Research Methodology

There are many systems, methods and algorithms for data measurement and analysis (Rymarczyk, 2021; Rymarczyk, 2019; Koulountzios, 2019; Korzeniewska, 2021; Korzeniewska 2021; Banasiak, 2014; Dusek and Mikulka, 2021; Kryszyn, 2019). The BSPM vest was constructed in such a way as to be able to measure the BSPM and EIT (Rymarczyk, 2019). For the EIT, we concluded that to reconstruct a 3D image, we need to include at least two rows of electrodes. These two rows are in the middle part of the vest, and the top two are located below the armpits (see Figure 1). The rest of the electrodes are located in such a way as to have a dense grid of electrodes around the patient's body. Also, the location of electrodes overlaps the points at which classical 12-lead ECG is performed; thus, the vest can measure standard ECG. The vest consists of 102 electrodes, all of which can be used for BSPM. In addition, the innovative design of the vest (shown in Figure 2) and the use of elastic textile-silicone electrodes (shown in Figure 3) allow for sound pressure and contact with the body and, consequently, better data reading.
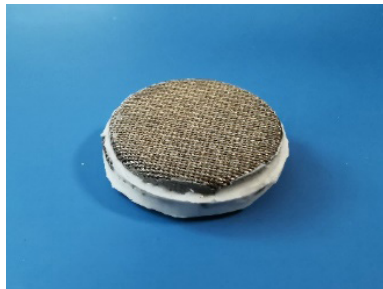
Figure 1. *The schematic view of the electrode location on the measuring vest*
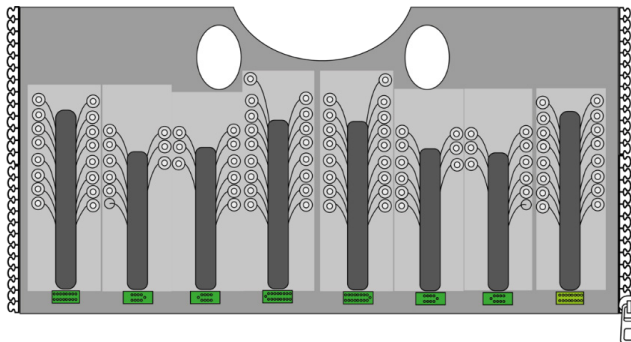
Figure 2. *The measuring vest was designed and manufactured by Netrix S.A.*

Figure 3. *The elastic silicone-textile electrode was designed and manufactured by Netrix S.A.*

The data for the analysis comes from the measurement signals simulation for the designed vest. The simulation system consisted of the following: The ProSim 4 ECG simulator generates an ECG-like signal for all standard and abnormal heart rhythms; the phantom is used to convert the 10-lead ECG simulator signal to 102 BSPM distributions. This was achieved by designing a net of resistors that mimicked the human body. Multiplexer systems are connected in series using FFC tape. A controller circuit board amplifies and converts signals from analogue to digital signals.

Due to the specifics of the measured signal (low signal-to-noise ratio, low signal amplitude), it was necessary to design and develop a custom filtering system to compare the measurements obtained to the state-of-the-art Holters. The simulator can generate a standard ECG signal, slow heart rate down to 30 BPM, increase heart rate up to 300 BPM, and various disorders such as atrial fibrillation, premature ventricular contraction, ventricular tachycardia, ventricular fibrillation, transvenous pacer pulse, second-degree AV block, third-degree AV block. The signal from the simulator is close to the natural heart rhythm – with a similar electrical amplitude level and type of noise. This device is used in hospitals to test and validate the correct operation of ECG monitors and other equipment used to monitor heart rhythm (Randazzo, 2022; Sadrawi, 2017).

A phantom was created to test the designed solution, converting signals from a 10-channel ECG simulator into a 128-channel potential distribution map compatible with the previously designed multiplexer blocks. Each measurement channel has an independent forming and pre-filtering system, thanks to which the signal fed to the analogue keys shows a much higher signal-to-noise ratio than the directly measured signal. Additionally, input blocks ensured the maximum input impedance of the measurement system. The schematic of the measurement step is shown in Figure 4.

**Figure 4.** *Diagram showing the measurement setup*

Figure 4 shows the schematic diagram corresponding to the experimental setup used during the data collection. On the Left, the FLUKE ProSim4 ECG signal simulator is visible. Fluke ProSim4 is used in hospitals for periodic validation of ECG devices. It is designed to test patient monitors at the point of use. The easy and secure connection ensures the simulator can test 12-lead ECG, NIBP, IBP and respiration in seconds. Built-in test sequences, intuitive operation and one-touch screen access to most functions make the ProSim 4 an indispensable diagnostic tool for evaluating the performance of monitoring devices. The ten leads from the simulator are connected to the phantom equipped with conduction copper pads. Inside the phantom is a network of resistors that mimic the human body's continuous resistance.

The simulated potentials are measured via removable elastic textile electrodes mounted on the vest. The signals are measured, filtered, and transmitted via USB or Wi-Fi to the computer for further analysis. The vest contains eight boards that can control the measurement of 128 channels. In the vest, only 102 are used. Each board is connected in series with the other. Finally, the last board is connected to the main EIT/BSPM board. The mainboard has the FPGA that controls electrical impedance (EIT) and BSPM. It is also equipped with Analog Digital Converters (ADC) and multiplexers. The collected data is then sent to the computer over a USB or Wi-Fi ESP32 module. The mainboard also has analog and software filters. The FPGA also plays a role in signal filtering. One of the board's goals is to deal with noise and baseline wander cancellation.

The system has been designed using analogue multiplexers coupled with filters and amplifiers that form the signal to values valid for measurements. The signal is formed after leaving the multiplexer block, and it is filtered again using an additional stopband filter cutting off 50Hz frequency and a combiner system using the resultant Wilson signal as a reference. It is passed on to ADC converters, where the last process of signal filtration takes place with the FFT filter. The measurement process is carried out cyclically on all 128 measured channels, thus obtaining an adequate sampling of the signal at the level of 1ksps.

The system was tested with the developed potential reconstruction algorithm, where the potential collected on the heart was simulated on the body. The inverse of that problem was also calculated where the potential on the heart is reconstructed from the measurement on the body, as shown in Figure 5.

Figure 5. *The electrical potential on the heart was reconstructed from the simulation of BSPM measurement*
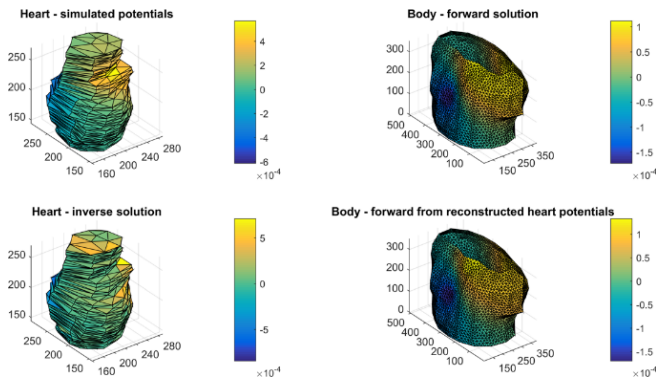
After leaving the multiplexer block, the signal is filtered with a band-stop filter cutting off 50Hz frequency and a combiner system using the resultant Wilson signal as a reference. Finally, such signal is passed from analogue to digital converters, where the last process of signal filtration takes place using the FFT filter. The measuring process occurs cyclically on all the available 128 measured channels, obtaining an adequate signal sampling at 1ksps. It is worth noting that although the system can measure 128 channels, only 102 were used for BSPM. The measured data is then transmitted via Ethernet to an IoT hub located on the company server cluster for analysis.

Signal simulations were performed with the following heart disorders: AFib_Fine – Atrial fibrillation; Bradycardia – heart rate below 60 times per minute; Normal – Normal sinus rhythm; PVC – Additional ventricular stimulation; Tachycardia – heart rate above 100 times per minute; VFib_Fine – Ventricular Fibrillation – suddenly attempt to contract at rates of up to 500 bpm; TachFine – Ventricular Tachycardia – broad complex tachycardia originating in the ventricles. Fragments of signals with disturbances are presented in 9.

Figure 6. *The BSPM vest measures the signals for a single channel. The signals presented are as follows: a) AFib_Fine, b) Brachycardia, c) Normal disturbance, d) PVC disturbance, e) Tachycardia, and f) VFib_Fine disturbance.*
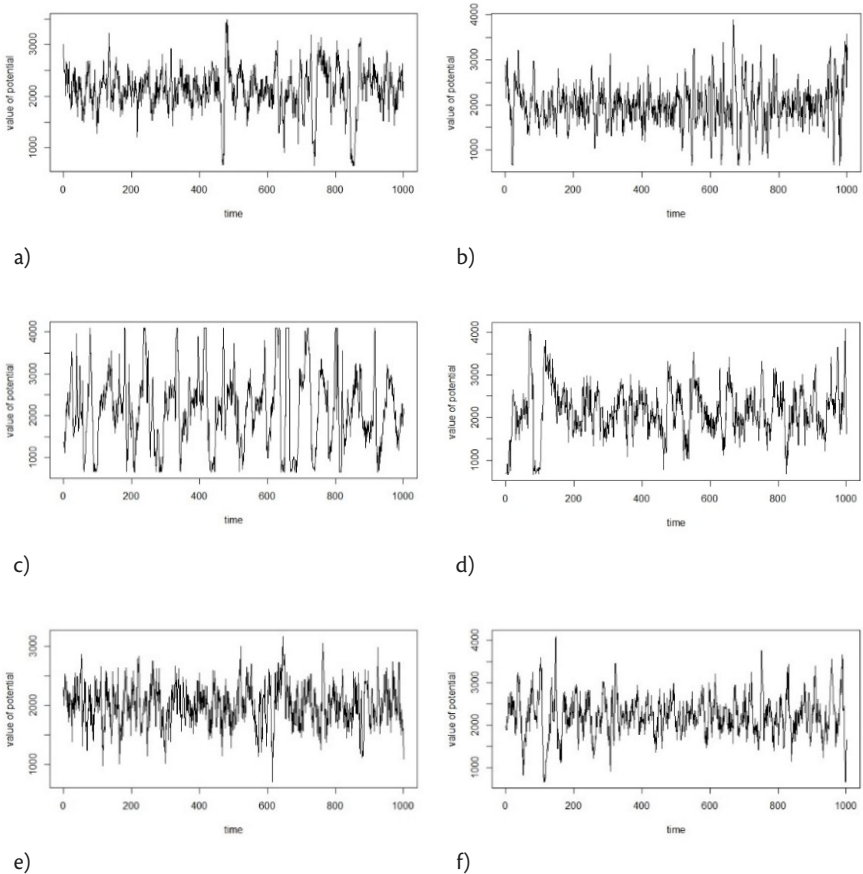
Principal component analysis (PCA) was used to find information relationships between channels (Jolliffe, 2002). Principal Component Analysis is a method of orthogonal linear transformation to a new system of variables. It consists in transforming the data matrix into a new coordinate system. Consider an X-data matrix with dimensions . In the X matrix, each column is a p-dimensional data vector from each sensor. Normalization is performed

on the columns to eliminate the differences between the possible differences among the values in the columns. This transformation is an l-dimensional set of p-dimensional weight vectors $w_{(k)} = (w_1, \ldots w_p)_{(k)}$, which converts the $x_{(i)}$ lines matrix X into new variables $PC_{(i)} = (PC_1, \ldots PC_l)_{(i)}$ provided by

$$PC_{k(i)} = x_{(i)} \cdot w_{(k)}, \ i = 1, \ldots, n \ \ k = 1, \ldots, l$$

RESEARCH METHODOLOGY

Statistical analyses and data visualisation were performed in an R environment using complot, factor extra, and ggplot2 libraries. A corrupt matrix from R was used to show the correlation between the channels in the signals and individual disorders. This matrix is created to visualise the correlation strength from the correlation matrix calculated for the channels. If the correlation is strongly positive, the given point showing the correlation between individual channels is marked as the navy-blue intensity. The correlation strength is shown as the red colour intensity if the correlation is negative.

Figure 7. *Corrplot diagram of the correlation matrix. Channel numbering starts at 1 for the upper-left corner of the matrix*

AFib_Fine disorder   VFib_Fine disturbance   VTach_Fine disturbance
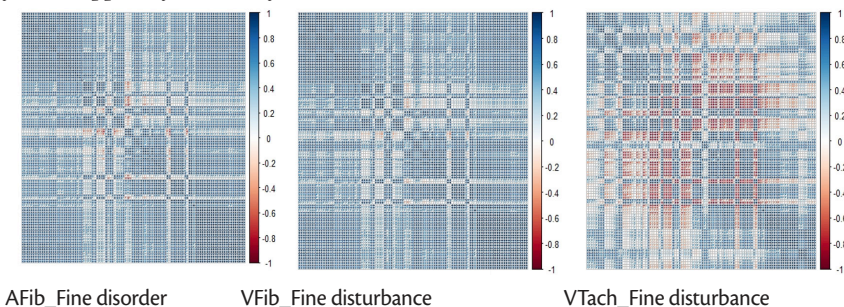
The correlation matrix structure is similar for AFib_Fine, Bradycardia, Normal, PVC, Tachycardia, and VFib_Fine disorders, as can be observed in Figures 6 and 7 b) 's correlation diagrams. Figure 10 c) shows the correlation matrix for the VTach_Fine disorder. The structure of the matrix differs significantly from that of other disorders.

PCA analysis was conducted for signals with individual disturbances to obtain latent variable (PC) channels in BSMP measurements. Measurement values from particular channels in BSPM measurements were taken as input variables in the PCA model. Separate analyses were performed for each disorder. After PCA analysis, a cumulative value for each disorder was obtained for the first two variables above 80% for PVC and 92% for VTach_Fine. For all the disorders, the cumulative value of the explained variance percentage is so significant that the first two variables represent the channel system. For both PC1 and PC2, the eigenvalues were more important than 1. Therefore, based on the Kaiser criterion and the percentage of explained variance criterion, two PC1 and PC2 have been chosen to represent the system.

**Table 1.** *Percentages of explained variance for individual PC variables for data from individual disorders*

Disorder	AFib_Fine	Bradycardia	Normal	PVC	Tachycardia	VFib-Fine	VTach_Fine
PC1	69%	68%	68%	63%	52%	67%	54%
PC2	18%	19%	18%	18%	36%	19%	38%

The distribution of factor loadings for AFib_Fine, Bradycardia, Normal, PVC, Tachycardia, and VFib_Fine disorders are similar. The distribution and intensity change slightly within a given disorder. For the VTach _Fine variable, the factor loadings distribution differs from the other variables. More channels have weaker factor loadings for the variable PC1, while more channels from PC2 have more substantial factor loadings. A detailed list of the relevant channels can be found in Table 2. Figure 8 and Figure 9 mark the electrodes for which significant components were obtained in the variable PC1 and PC2 for the standard signal.

Table 2. *Significant channels for the standard signal are divided into PC1 and PC2 variables*

	Normal Signal	Negative factor loadings	Positive factor loadings
PC1	High	1-16, 19-25, 27, 28, 33, 39, 42, 47, 52-55, 59, 61-63, 70-72, 75, 78, 80-102	
	Medium	17,18, 26, 34, 41, 44-46, 51, 56, 58, 60, 64, 65, 69, 73, 74, 77	
	Insignificant	29-32, 35-38, 40, 43, 48-50, 57, 67-68, 76, 79	
PC2	High	17, 26, 29-32, 35-38, 43-46, 67-68,	34, 40, 41, 48-51, 56-58, 60, 61, 63-66, 69
	Medium	18,19	
	Insignificant	1-16, 20-25, 27-28, 33, 39, 42, 52-55, 59, 62, 66, 71, 72, 78-102	

Figure 8. *PC1 for VTachFine disturbance (dark blue point – high impact negative coefficient, blue – medium impact negative coefficient)*
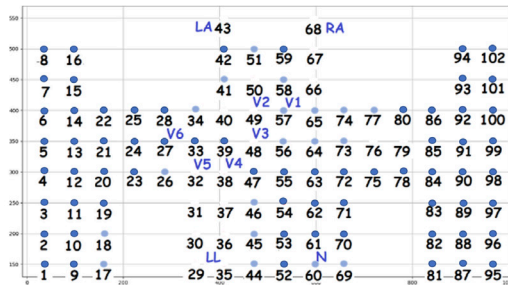
Figure 9. *PC 2 for VTachFine disturbance (dark blue point – high impact negative coefficient, Redpoint – high impact positive coefficient)*
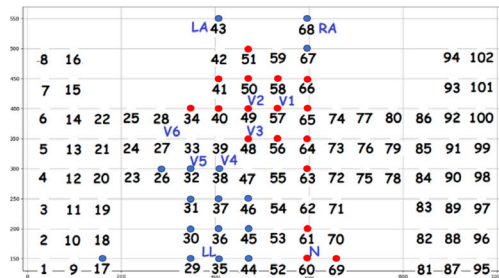
For all disorders other than VTach_Fine, the channels' information differences vary only in a few channels, mainly on the PC2 variable. The differences in the channels to the standard signal are presented in Table 3.

Table 3 *shows differences in the significance of channels to the signal without disturbance for the PC1 and PC2 variables*

|		Additional significant channels compared to normal	Channels insignificant compared to normal
PC1	AFib_Fine	lack	lack
	Bradycardia	lack	lack
	PVC		41, 44, 45, 56, 58, 60
	Tachycardia	79	9, 17-20, 23-24, 26-27, 44-46, 75
	VFib_Fine		56, 60, 75
PC2	AFib_Fine	23,72	
	Bradycardia	23,75	
	PVC	9, 20	
	Tachycardia	1-4, 9-13, 20-21, 24, 27, 33, 47	69
	VFib_Fine		75

In the case of VTach_Fine disturbance, due to the similar percentages of PC1 and PC2 variable inputs in the system of variables, significant factor loadings in PC1 and PC2 are changed. Table 5 shows the significance of the channels for the VTach_Fine disorder in terms of variables.

Table 5. *Significant channels for the signal with VTach_Fine disturbance divided into PC1 and PC2 variables*

VTachFine		Negative factor loadings	Positive factor loadings
PC1	High	29-32, 35-38, 43-45, 67-68, 76	15, 34, 39-41, 48-51, 55-56, 69-74, 77-86, 91-94, 101-102
	Medium	17-19, 26, 46, 75	7,8, 16, 52, 87-90, 99-100
	Insignificant	1-6, 9-14, 20-25, 27-28, 33, 42, 47, 53-54, 95-98	
PC2	High		1-6, 9-14, 17-28, 33, 42, 45-47, 52-54, 75, 87-90, 95-100
	Medium		7,8, 16, 29-32, 36, 44, 67, 91-94, 101-102
	Insignificant	15, 34, 35, 37-41, 43, 48-51, 55-66, 68-74,76-86	

Figures 10 and 11 mark the electrodes for which significant components were obtained in the variables PC1 and PC2 for the signal with VTachFine disturbance.

Figure 10. *PC1 for VTachFine disturbance (dark blue point – high impact negative coefficient, blue – medium impact negative coefficient, Redpoint – high impact positive coefficient, yellow – medium impact positive coefficient)*
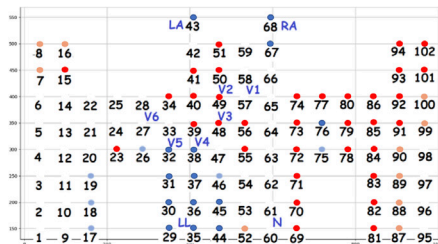
Figure 11. *PC2 for VTachFine disturbance (dark blue point – high impact negative coefficient, blue – medium impact negative coefficient)*
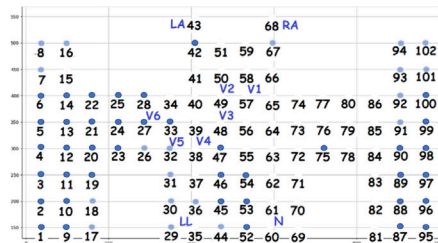
DISCUSSION

We analysed differences in the significance of the factor loadings for individual disturbances compared to the standard signal. For AFib_Fine, Bradycardia, Normal, and Tachycardia VFib_Fine disorders, the structure of significant channels in the PC1 and PC2 variables was similar.

For the PC1 variable, channel 79 was an additional important channel in the tachycardia disorder. In addition, channels 41, 44, 45, 56, 58, and 60 (Table 3) from the front left lower and upper left chest appeared insignificant in the PVC disturbance compared to the standard signal. For the PC1 variable for Tachycardia disorder, the channels lying on the left side and symmetrically placed channel 75 on the right side turned irrelevant compared to the signal without the disorder.

For the VFib Fine variable, these are channels 56, 60, and 65. The channel structure in the PC2 variable is more diverse than in the PC1 variable except for the VTach_Fine disorder, which, due to the most similar values of the percentage of explained variance of Variables PC1 and PC2, where the roles of the factors change places.

The main channels responsible for disturbance are those associated with a classical ECG measurement system with 12 channels labelled in Figure 8-11. Most of these channels are not significant in the PC1 variable but essential in PC2. This means that the PC1 variable will contain the information core of the similarities between the channels. The PC2 variable, on the other hand, will include information about specific disturbances in the BSPM signal. The main difference in the significance of the PC2 variable is that the channels on the left side and left back are essential for the Tachycardia disorder. Additional important channels are under the left armpit for AFib_Fine, PVC, and Brachycardia disorders.

For the variable VTach _Fine, probably by the most similar values of the percentage explanation of the channel system, the factor loadings in the variables PC1 and PC2 are exchanged with each other to the signal without disturbance. There is also a more differentiated division into channels with positive and negative factor loadings, which results in a more significant differentiation of the signs of loadings for both PC1 and PC2 than other disturbances. For the VTach Fine disorder for the PC1 variable, the important

channels are those in the upper right and lower left front of the chest and the right side and right back.

The main factor containing information about disturbances in the conducted analysis is the PC2 factor, which determines the channels responsible for distinguishing disorders. The exception is the VTach_Fib disorder, where due to similar percentage values of explained variance of PC1 and PC2 variables, the PC2 variable is a variable with a similar structure to the PC1 variables from the remaining disorders. Therefore, for a VTach_Fine disorder, the PC1 variable will be responsible for channel differentiation for this disorder.

The differences between the Vtach Fine signal and the others are most likely due to the specifics of the signal itself. The VtachFine signal shows that the factors that enter PC1 and PC2 are swapped. Figure 7c shows a higher correlation between the channels (the vectors responsible for the channels are more concentrated), so these visitors will have higher factor charges and carry more information about PC1. Hence, there is also a higher percentage of explained variance in the PC1 variable compared to the other disturbances.

Conclusion

The paper presents research on determining information dependencies in the BSPM measurement channels. First, based on the simulation system constructed for testing the innovative BSPM measuring waistcoat, heart rhythm signals were performed with disorders: Atrial fibrillation, Bradycardia, Normal signal, PVC, Tachycardia, Ventricular Fibrillation, Ventricular Tachycardia. Then, the connections between measurement channels were indicated using the PCA method, and latent variables, grouping individual measurement channels (electrode signals), were specified. Two new latent variables, PC1 and PC2, were selected for individual disturbances and standard signal, following the Kaiser criterion and the percentage of explained variance. Based on the number of electrodes in the waistcoat coinciding with the classical ECG electrodes, it was indicated that the variable PC2 is the variable based on which a particular disturbance is identified. The exception is the VTachFine disturbance for which variable PC1 is shown.

The PCA analysis conducted in this paper has two tasks. The first is data reduction. Determining latent variables by PCA results reduced the data dimension from 102 variables in measurement data from the measuring electrodes to 2 variables, PC1 and PC2. In addition to data reduction, PCA also has the advantage of getting rid of measurement noise and irrelevant variables without removing variables but only parts of them. The second is mapping areas on the patient's body for significant measurement electrodes, which can be determined from significant factor loadings in the latent variables PC1 and PC2. Such areas can be helpful during the detection of disease areas, e.g., electrodes during ECG measurement can be applied in other regions than classically used in ECG. A disadvantage of the PCA method is its sensitivity to measurement signal disturbances. Therefore, a distortion-free, filtered, or pre-filtered signal is needed. The authors will extend this research by showing how the indicated areas on the patient's body correlate with regions in the heart, which will result in a very detailed diagnosis.

The work presented here is used in a cloud expert system that analyses and classifies EIT and BSPM signals. It is currently patented (patent no. 437101).

The research will also be the basis for validating clinical studies conducted on patients, where additional problems may arise due to signal interference caused by electrode friction, improper adhesion of electrodes to the patient's body, or patient movement during the test.

REFERENCES

Banasiak, R., Wajman, R., Jaworski, T., Fiderek, P., Fidos, H., Nowakowski, J., Sankowski, D. (2014). Study on two-phase flow regime visualisation and identification using 3D electrical capacitance tomography and fuzzy-logic classification. Int. J. Multiph. Flow, 58, s. 1–14.

Bonizzi, P. Guillem, M., Castells, F., Climent A., Zarzoso V. (2009). Significance of mixing matrix structure on principal component-based analysis of atrial fibrillation body surface potential maps, Computers in Cardiology, 41-44.

Castells F., Laguna P., Sornmo L., BollmannA., Roig J.G. (2007). Principal Component Analysis in ECG Signal Processing, Hindawi Publishing Corporation EURASIP Journal on Advances in Signal Processing, 21, 074580, doi:10.1155/2007/74580

Daly, M.J., Finlay, D.D., Scott, P.J., Nugent, C.D., Adgey, A. J., Harbinson, M.T. (2013). Pre-Hospital Body Surface Potential Mapping Improves Early Diagnosis of Acute Coronary Artery Occlusion in Patients with Ventricular Fibrillation and Cardiac Arrest. Resuscitation, 84, 37–41, doi:10.1016/j.resuscitation.2012.09.008

Donnelly, M. P., Nugent, C. D., Finlay, D. D., Rooney, N. F., Black, N. D. (2006). Diagnosing Old MI by Searching for a Linear Boundary in the Space of Principal Components, IEEE Transactions on Information Technology in Biomedicine, 10(3), 476-483, doi: 10.1109/TITB.2006.876033

Dusek, J., Mikulka, J. (2021). Measurement-Based Domain Parameter Optimization in Electrical Impedance Tomography Imaging, Sensors, 21(7), 2507; https://doi.org/10.3390/s21072507

Hänninen, H., Takala, P., Rantonen, J., Mäkijärvi, M., Virtanen, K., Nenonen, J., Katila, T., Toivonen, L. (2003). ST-T Integral and T-Wave Amplitude in Detection of Exercise-Induced Myocardial Ischemia Evaluated with Body Surface Potential Mapping. J Electrocardiol, 36, 89–98, doi:10.1054/jelc.2003.50013

Hoekema, R., Gurlek, C., Brouwer, M.A., Chaikovsky, I., Verheugt, F.W.A. (2004). The Use of Magnetocardiography and Body Surface Potential Mapping in the Detection of Coronary Artery Disease in Chest Pain Patients with a Normal Electrocardiogram. In Proceedings of the Computers in Cardiology, 2004; 389–392.

Jolliffe, I.T. (2002). Principal Components in Regression Analysis. In Principal Component Analysis; Ed.; Springer Series in Statistics; Springer: New York, NY, 167–198. ISBN 978-0-387-22440-4.

Kłosowski, G., Rymarczyk, T., Wójcik, D., Skowron, S., Cieplak, T., Adamkiewicz, P. (2020). The Use of Time-Frequency Moments as Inputs of LSTM Network for ECG Signal Classification. Electronics 2020, 9, s. 1452, doi:10.3390/electronics9091452.

Korhonen, P., Husa, T., Konttila, T., Tierala, I., Mäkijärvi, M., Väänänen, H., Toivonen, L. (2009). Complex T-Wave Morphology in Body Surface Potential Mapping in Prediction of Arrhythmic Events in Patients with Acute Myocardial Infarction and Cardiac Dysfunction. EP Europace, 11, 514–520, doi:10.1093/europace/eup051

Korzeniewska, E., Krawczyk, A., Stando, J. (2021). Torsion field – an example of pseudo-scientific concept in physics, Przeglad Elektrotechniczny, Volume97, Issue1, Page196-199, DOI10.15199/48.2021.01.41

Korzeniewska, E., Szczesny, A., Lipinski, P., Drozdz, T., Kielbasa, P., Miernik, A. (2021). Prototype of a Textronic Sensor Created with a Physical Vacuum Deposition Process for Staphylococcus aureus Detection, SENSORS Volume: 21 Issue: 1 Article Number: 183 DOI: 10.3390/s21010183

Koulountzios, P., Rymarczyk, T., Soleimani, M. (2019). A quantitative ultrasonic travel-time tomography system for investigation of liquid compounds elaborations in industrial processes, Sensors, vol. 19, no. 23, 5117.

Kryszyn, J., Wanta, D., Smolik, W. T. (2019). Evaluation of the electrical capacitance tomography system for measurement using 3d sensor. Informatyka, Automatyka, Pomiary W Gospodarce I Ochronie Środowiska,, 9(4), 52-59.

Lux, R.L. (2010). Body Surface Potential Mapping Techniques. In Comprehensive Electrocardiology; Macfarlane, P.W., van Oosterom, A., Pahlm, O., Kligfield, P., Janse, M., Camm, J., Eds.; Springer: London, 1361–1374. ISBN 978-1-84882-046-3.

Patent no P.437101, https://ewyszukiwarka.pue.uprp.gov.pl/search/pwp-details/P.437101

Polak-Jonkisz, D., Laszki-Szczachor, K., Purzyc, L., Zwolińska, D., Musiał, K., Pilecki, W., Rusiecki, L., Janocha, A., Kałka, D., Sobieszczańska, M. (2009). Usefulness of Body Surface Potential Mapping for Early Identification of the Intraventricular Conduction Disorders in Young Patients with Chronic Kidney Disease. J Electrocardiol, 42, 165–171, doi:10.1016/j.jelectrocard.2008.09.007

Potse M., Puyo S., Bear L., Hocini M., Ha¨ıssaguerre M., Dubois R. (2017). Non-Invasive Assessment of Spatiotemporal Organization of Ventricular Fibrillation Through Principal Component Analysis, Computing in Cardiology, 44, doi:10.22489/CinC.2017.101-051

Przysucha, B., Rymarczyk, T., Wójcik, D., Wos, M., Vejar, A. (2020). Improving the Dependability of the ECG Signal for Classification of Heart Diseases.; IEEE Computer Society, 63–64.

Randazzo, V., Ferretti, J., Pasero, E. (2021). Anytime ECG Monitoring through the Use of a Low-Cost, User-Friendly, Wearable Device. Sensors, 21, 6036, doi:10.3390/s21186036

Robinson, M.R., Curzen, N. (2009). Electrocardiographic Body Surface Mapping: Potential Tool for the Detection of Transient Myocardial Ischemia in the 21st Century? Ann Noninvasive Electrocardiol , 14, 201–210, doi:10.1111/j.1542-474X.2009.00284.x

Rodrigo, M., Climent, A., Liberos, A., Fernández-Aviles, F., Atienza, F., Guillem, M., Berenfeld, O. (2017). Minimal Configuration of Body Surface Potential Mapping for Discrimination of Left versus Right Dominant Frequencies during Atrial Fibrillation. Pacing and Clinical Electrophysiology , 40, 940–946, doi:10.1111/pace.13133

Rymarczyk, T., Kłosowski, G., Hoła A., Sikora, J., Wołowiec, T., Tchórzewski, P., Skowron, S. (2021). Comparison of Machine Learning Methods in Electrical Tomography for Detecting Moisture in Building Walls, Energies, 14(10), 2777.

Rymarczyk, T., Nita, P., Vejar, A., Woś, M., Stefaniak, B., Adamkiewicz, P. (2019). Wearable Mobile Measuring Device Based on Electrical Tomography. Electrotechnical Review, 1, 213–216, doi:10.15199/48.2019.04.39

Rymarczyk, T., Stanikowski, A., Nita, P. (2019). Wearable sensor array for biopotential measurements. Applications of Electromagnetics in Modern Engineering and Medicine (PTZE),184–187.

Rymarczyk, T., Woś, M., Bartosik, M., Vejar, A., Kozłowski, E., Maj, M. (2020). Electrical Activity with ECG Analysis for Body Surface Potential Mapping. Electrotechnical Review R. 96, nr 10, s. 144–147, doi:10.15199/48.2020.10.26

Sadrawi, M., Lin, C.-H., Lin, Y.-T., Hsieh, Y., Kuo, C.-C., Chien, J.C., Haraikawa, K., Abbod, M.F., Shieh, J.-S. (2017). Arrhythmia Evaluation in Wearable ECG Devices. Sensors (Basel), 17, 2445, doi:10.3390/s17112445

Simelius, K., Stenroos, M., Reinhardt, L., Nenonen, J., Tierala, I. Mäkijärvi, M., Toivonen, L., Katila, T. (2003). Spatiotemporal Characterization of Paced Cardiac Activation with Body Surface Potential Mapping and Self-Organizing Maps. Physiol. Meas., 24, 805–816, doi:10.1088/0967-3334/24/3/315

SippensGroenewegen, A., Lesh, M.D., Roithinger, F.X., Ellis, W.S., Steiner, P.R., Saxon, L.A., Lee, R.J., Scheinman, M.M. (2000). Body Surface Mapping of Counterclockwise and Clockwise Typical Atrial Flutter: A Comparative Analysis with Endocardial Activation Sequence Mapping. J Am Coll Cardiol, 35, 1276–1287, doi:10.1016/s0735-1097(00)00549-0

Zarychta, P., Smith, F.E., King, S.T., Haigh, A.J., Klinge, A., Zheng, D., Stevens, S., Allen, J., Okelarin, A., Langley, P., et al. (2007). Body Surface Potential Mapping for Detection of Myocardial Infarct Sites. In Proceedings of the 2007 Computers in Cardiology; 181–184.

Weber, F. M., Keller, D. U. J., Bauer, S., Seemann, G., Lorenz, C., Dössel, O. (2011). Predicting Tissue Conductivity Influences on Body Surface Potentials—An Efficient Approach Based on Principal Component Analysis, IEEE Transactions on Biomedical Engineering, 58(2), 265–273. doi:10.1109/tbme.2010.2090151

Wójcik, D., Kozłowski, E., Woś, M., Rymarczyk, T., Wośko, E. (2020). Machine Learning Pathology Detection with a Body Surface Potential Mapping. In Proceedings of the Adjunct Proceedings of the 2020 ACM International Joint Conference on Pervasive and Ubiquitous Computing and Proceedings of the 2020 ACM International Symposium on Wearable Computers; Association for Computing Machinery: New York, NY, USA, September 10, 151–155.